Feature Preserving SAR Despeckling and Its Parallel Implementation with Application to Railway Detection

O. Erman Okman[1], Fatih Nar[1], Can Demirkesen[1], [1]Space and Defence Technologies Inc., Turkey
Müjdat Çetin[2], [2]Faculty of Engineering and Natural Sciences, Sabancı University, Turkey

Abstract

We consider the problem of despeckling synthetic aperture radar (SAR) images and propose an approach we call feature preserving despeckling (FPD). FPD is obtained through the adoption of a regularized SAR image reconstruction algorithm for the despeckling problem. FPD performs smoothing of homogeneous regions while preserving strong scatterers as well as region boundaries. We implement FPD in CUDA for fast parallel processing. We evaluate the performance of FPD through its impact on the performance of railway detection. To this end, we propose a semi-automated algorithm for railway detection in SAR images. We compare the performance of FPD to well-known despeckling methods and demonstrate the improvements it provides for railway detection.

1 Introduction

Because of the all weather and all time capabilities of Synthetic Aperture Radar (SAR) imaging sensors, SAR images have become very popular for many different remote sensing applications from land cover/use classification to automatic target recognition (ATR). However, SAR images, like other coherent imaging modalities, suffer from speckle noise, which is a multiplicative and locally correlated noise. Speckle noise makes the interpretation of the objects difficult. Hence, for many target detection and recognition problems, the very first step is removal of the speckle. To this end, the main goal of speckle reduction algorithms is to remove the speckle while keeping the details of the targets in the scene.

In the literature, there are many adaptive filtering algorithms to achieve this purpose. Lee proposed a method which evaluates the output image by a linear combination of the center pixel of the defined window and the average intensity in that window [1]. Kuan et al. also proposed a very similar approach but using a different signal model [2]. Frost filter is based on an exponential kernel whose parameters include the local coefficient of variation [3]. Hence, the filter is in between an all pass filter and an averaging filter depending on the coefficient of variation in the kernel window. Lopes et al. introduced some modifications to Lee and Frost filters by use of two thresholds on the coefficient of variation [4]. In that study, it is observed that the filter response is adequately averaging for homogenous regions while keeping the details in edgy and textured regions with respect to the original forms of the filters. Lopes et al. also proposed some modifications to Kuan filter by assuming Gamma distributed scene reflectivity and setting up two thresholds [5].

In [6], image denoising is achieved by combining wavelet Bayesian denoising with an image regularization technique based on Markov random fields (MRF). Sveinsson et al., proposed to use total variation segmentation to combine time invariant wavelet and curvelet transforms for despeckling of an image since wavelet transform provides better smoothing in homogenous regions and curvelet transform provides better denoising in regions with edges [7]. In [8], speckle is reduced using a MRF approach where total variation minimization is also utilized to smooth homogeneous regions while preserving sharp transitions.

Another approach for SAR image despeckling is to use diffusion based methods. Speckle reducing anisotropic diffusion (SRAD) [9], is one of the most popular diffusion based approaches and basically it is an edge sensitive extension of the Lee and Frost filters. In that study, the original anisotropic diffusion proposed in [10] is extended for removal of the spatially correlated multiplicative noise. Krissian et. al extended this approach by allowing different levels of filtering across the image contours and in the directions of principal curvature [11]. Pollak et al. proposed a method for edge enhancement and segmentation using stabilized inverse diffusion equations [12].

In [13], a method for reconstruction of spotlight mode SAR images while enhancing some of the features in the scene has been proposed. Just like previously mentioned methods involving total variation regularization and anisotropic diffusion, the method in [13] also produces images exhibiting smooth regions and preserved edges while enhancing the bright scatterers. The re-

construction problem is defined as an optimization problem and a quasi-Newton method built upon half quadratic regularization is proposed to solve this problem.

The first contribution of our study is to adopt the approach in [13], for despeckling of SAR images. The experiments show that the method produces very promising results. To remedy high computational load of the proposed method efficient parallel implementation is realized on Nvidia GPUs using CUDA. For many of the applications, these methods are used as a preprocessing step of an automatic image interpretation operation. Hence, it is very important to determine the effects of a despeckling approach on the image interpretation task, such as object detection or recognition. However, in the literature, despeckling methods are usually evaluated based on a number of metrics defined on the despeckled images. In this study, we quantitatively evaluate edge preserving despeckling methods and compare their performance in terms of their impact on automatic target detection. Since railways appear as long and thin structures like bright edges in SAR images, these structures are selected as the target of interest and detection results of railways are the measure of the success for filters used.

In Section 2, the proposed despeckling filter is discussed. The proposed railway detection algorithm is explained in Section 3. Section 4 contains the results of the experiments performed and lastly Section 5 concludes the paper.

2 Feature Preserving Despeckling (FPD) Filter

In [13], the SAR image reconstruction problem is posed as an optimization problem:

$$\hat{f} = \arg\min_{f} J(f) \tag{1}$$

where the objective function *J(f)* is defined as:

$$J(f) = \|g - Tf\|_2^2 + \lambda_1^2 \|f\|_k^k + \lambda_2^2 \|D|f\|_k^k \tag{2}$$

where g is the SAR range profile observations, T is the transformation representing the SAR projection operator, $\|.\|_k$ denotes the l_k norm, D is the 2-D derivative operator, f is the noise free reflectance image of the scene, and λ_1 and λ_2 are scalar parameters. The first term of the objective function is the fidelity term; the second and third terms are for enhancing point based and region based features, respectively. In this study, we adopt this method for despeckling of the real-valued SAR images thus edges and bright points are preserved while homogeneous regions are smoothed.

In our case, g is the observed speckled image, f is the smoothed image and T is equal to identity matrix. Following [13], we solve this problem using a quasi-Newton algorithm given in Equation (3) based on the Hessian approximation in Equation (5).

$$f^{n+1} = f^n - \left[\widetilde{H}\left(f^n\right)\right]^{-1} \nabla J_m\left(f^n\right) \tag{3}$$

where

$$\nabla J_m\left(f^n\right) = \widetilde{H}\left(f^n\right) f^n - 2g \tag{4}$$

and

$$\widetilde{H}\left(f^n\right) \triangleq 2I + k\lambda_1^2 \Lambda_1\left(f^n\right) + k\lambda_2^2 D^T \Lambda_2\left(f^n\right) D \tag{5}$$

$$\Lambda_1\left(f^n\right) \triangleq diag\left\{\left[\left(f^n\left(x_i, y_i\right)\right)^2 + \varepsilon\right]^{\frac{k}{2}-1}\right\}$$

$$\Lambda_2\left(f^n\right) \triangleq diag\left\{\left[\left(\nabla f^n\left(x_i, y_i\right)\right)^2 + \varepsilon\right]^{\frac{k}{2}-1}\right\}$$

When Equation (4) is substituted into Equation(3), a linear system of equations is obtained and it is solved using the conjugate gradient (CG) method as in [13].

2.1 CUDA Implementation of FPD

Matrix operations in Equation (5) are divided into 6 filtering operations which only involve local computations on the pixels themselves and their right and bottom neighbors. These operations consist of 3 if conditions, 3 + 3 global memory reads from two arrays, 3 global atomic memory writes, 3 power, 3 square, 9 multiplication, 20 division, 13 addition, 16 subtraction, and 4 conditional assignment operations. Remaining computational parts are composed of vector operations such as transpose and Euclidean distance. These operations are efficiently implemented in CUDA where parallel reduction is used for calculating dot product, norm, and Euclidean distance operations. The computational efficiency of the CUDA implementation can be seen in Table 1.

Table 1. Durations and processor occupancies of different FPD filter implementations for a 2000x2000 16 bit SAR image

Language	Precision	Parallel	Time (s)	Occupancy
Matlab	double	8 threads	1300	65.0%
C++	double	8 threads	295	100.0%
C++	single	1 thread	824	12,5%
C++	single	8 threads	206	100.0%
CUDA	single	336 core	16	80.0%

Analyses show that differences between the results of single and double precision implementations are very subtle hence single precision should be preferred due to its time and space efficiency. 8 threads C++ implementation is 4 times and Nvidia CUDA implementation is 51 times faster compared to single thread C++ implementation. Matlab and C++ (OpenMP) implementations are executed on i7, 3Ghz Intel CPU using 8 threads and CUDA implementation is executed on Nvidia GTX 460 GPU.

3 Railway Detection

In SAR images, railways appear as bright curves with different widths depending on the number of lines in the path. However, because of high speckle, the miss detection and false alarm rates are very high using simple curve detection methods. As a result, despeckling becomes crucial for effective railway detection.

In this study, a semi-automatic railway detection procedure is proposed. In this method, railways are approximated with short line segments hence the goal is to find connected line segments whose widths and orientations change smoothly beginning from the given initial point.

For line detection a modified version of the ratio line detector (RLD) proposed in [14] is used. In this method, a set of operations is defined in a kernel which gives high response to existing lines and this kernel is rotated in order to find lines in different orientations. For detecting a vertical line, the kernel shown in Figure 1 is used. In this kernel, three mean values (μ_A, μ_B, and μ_C) for the three regions shown in the figure are evaluated and the output of the RLD for the pixel at (x,y) is obtained using Equation (6):

$$\rho(x,y)=\left(1-\min\left\{\frac{w_B\mu_B+w_C\mu_C}{\mu_A(w_B+w_C)},1\right\}\right)\cdot\left(\min\left\{\frac{\mu_A}{I_{max}},1\right\}\right) \quad (6)$$

where w_A, w_B, and w_C indicate the widths of the three regions, and Imax is an arbitrary bright intensity value selected here as 255.

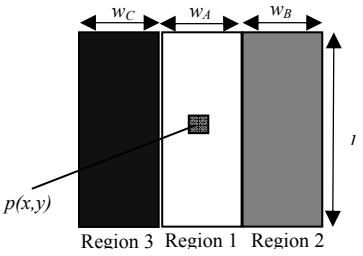

Figure 1. Line detector kernel with angle θ = 90°

For detection of the railways, after a point is selected by the user, the best initial point, which maximizes the function given in Equation (6), is searched around an MxM neighbourhood of the user selected point by changing the length of w_A and the angle of the kernel, θ. Hence, the initial point (x_0,y_0), initial line width $w_{A,0}$ and the initial direction of the line, θ_0, is obtained. Then, for each direction θ_n and $-\theta_n$ the following operations are carried out:

1. N lines are obtained which pass through the last found point at (x_n,y_n) and which uniformly sample the orientation space $\theta_n \pm \alpha/2$. Then, K points are uniformly sampled from each of the lines to be tested (Figure 2).

2. ρ in Equation (6) is evaluated for each black point given in Figure 2 and the point with maximum response, (x'_{n+1},y'_{n+1}), is found. Note that, for each point the angle of the kernel is the angle between that point and (x_n,y_n).

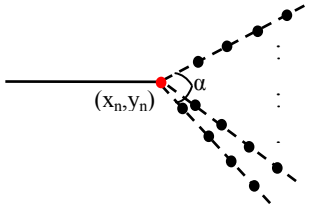

Figure 2. Test point selection for railway growing method (red point: last found, black points: to test)

3. Operation is terminated if $\rho(x'_{n+1},y'_{n+1})$ is smaller than a pre-determined threshold τ_ρ.

4. The next railway point is determined as:

$$\begin{bmatrix}x_{n+1}\\y_{n+1}\end{bmatrix}=\begin{bmatrix}x_n\\y_n\end{bmatrix}+d\begin{bmatrix}\cos(\theta_{n+1})\\\sin(\theta_{n+1})\end{bmatrix} \quad (7)$$

where

$$\theta_{n+1}=\beta\alpha_n+(1-\beta)\theta'_{n+1} \quad and \quad \beta=1-\frac{\rho(x'_{n+1},y'_{n+1})}{\rho(x_0,y_0)}$$

where θ'_{n+1} is the angle between points (x'_{n+1},y'_{n+1}) and (x_n,y_n) and the iterations are repeated from Step 1.

4 Experimental Results

We perform experiments to analyze the performance of the FPD filter presented in this paper and compare that with Enhanced Lee [1], Enhanced Frost [3] and SRAD [9] filters. The successes of these approaches are defined in terms of the success of the railway detection. In particular, we define a measure of success based on the cost function in Equation (6) as described below.

For each filtering method, the mean values of ρ 's are evaluated for all railway pixels and for the pixels less than 7 pixel distance to the railways, i.e., $\mu_{\rho,r}$ and $\mu_{\rho,n}$, respectively. Then, for a despeckling method, the success measure is defined as:

$$M_m=\mu_{\rho,r}-\mu_{\rho,n} \quad where \quad m\in\{Org,Lee,Frost,SRAD,FPD\} \quad (8)$$

Experiments are performed for nine images containing about 20 km of railways. The parameters of the filters are set after many trials. For the Enhanced Lee filter the kernel width is 7, the number of looks is 1, and damping is 1; for the Enhanced Frost filter the kernel width is 7, and damping is 1; for SRAD the number of iterations is set as 100, and for FPD λ_1 is 8, λ_2 is 16, and k is 1. The results can be seen in Table 2. The results show that FPD has larger measure values for most of the images which suggests that the proposed filter exhibits better noise removal and edge preservation characteristics while enhancing the contrast between the regions. Hence, for detection of the railways the method presented in this paper is more suitable

than the other despeckling approaches.

Table 2. Success measures (M_m) for FPD, Frost, Lee, SRAD filters, and the original image

	FPD	Frost	Lee	SRAD	Original
Image 1	0.19	0.21	0.16	0.18	0.14
Image 2	0.31	0.29	0.26	0.24	0.19
Image 3	0.30	0.26	0.29	0.22	0.15
Image 4	0.40	0.36	0.38	0.30	0.21
Image 5	0.25	0.24	0.25	0.23	0.20
Image 6	0.32	0.33	0.33	0.29	0.21
Image 7	0.16	0.15	0.15	0.15	0.14
Image 8	0.16	0.17	0.18	0.16	0.13
Image 9	0.09	0.09	0.09	0.09	0.09
M_m values	0.24	0.23	0.23	0.21	0.16

Moreover, the whole railway detection algorithm is executed for the same initial point on despeckled images obtained by different methods. Figure 3 shows our results on one of images used in our experiment. Visual analysis of these results also supports the point that the proposed railway detection method provides better results when used in conjunction with FPD.

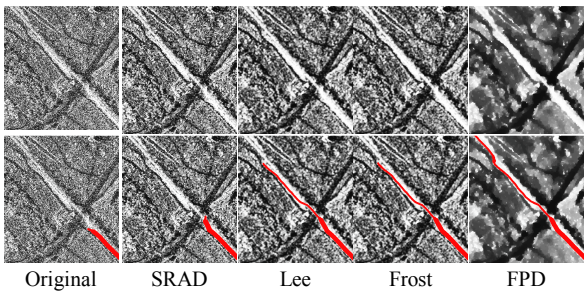

Figure 3. Different despeckling results (top) and corresponding railway detections (bottom)

5 Conclusion

In this study, a method for SAR image reconstruction is adopted for despeckling and implemented in CUDA to reduce its execution time. Besides, we proposed a semi interactive railway detection algorithm. Since the success of this algorithm relies on the success of initially used despeckling approach, experiments have been performed for different methods in the literature. The results show that the proposed despeckling algorithm is better for railway detection since it preserves edges and removes the speckle while enhancing the bright pixels on the railways due to the point feature enhancement characteristics it possesses. In future work, the railway detection method can be fully automated by extracting initial points. We are also planning to increase the speed of the CUDA implementation of the FPD filter by coalescing memory accesses, and increasing occupancy.

Acknowledgements

The authors thank Tolga Bölükbaşı for his support in implementation of the proposed filter.

References

[1] Lee, J. S.: *Speckle Suppression and Analysis for Synthetic Aperture Radar.* Practical Engineering, vol. 25, no. 5, pp. 636-643, 1986.

[2] Kuan, D., Sawchuk, A., Strand, T., Chavel, P.: *Adaptive Restoration of Images with Speckle.* IEEE T. Acoustics, Speech and Signal Processing, vol. 35, Issue 3, pp. 373-383, 1987.

[3] Frost V. S., Stiles, J. A., Shanmugan, K., S., Holtzman, J. C.: *A Model for Radar Images and Its Application to Adaptive Digital Filtering of Multiplicative Noise.* IEEE T. PAMI, vol. 4, pp. 157-165, 1987.

[4] Lopes, A.,Touzi, R, Nezry, E: *Adaptive Speckle Filters and Scene Heterogeneity*. IEEE T. Geosci Remote, vol. 28, pp. 992-1000, 1990.

[5] Lopes, A., Nezry, E., Touzi, R., and Laur, H.: *Structure detection and statistical adaptive speckle filtering in SAR images*. Int. J. Remote Sensing, vol. 14, no. 9, pp. 1735–1758, 1993.

[6] H. Xie, L.E. Pierce, and F.T. Ulaby, *SAR Speckle Reduction Using Wavelet Denoising and Markov Random Field Modeling*. IEEE T Image Process, vol. 40, pp. 2196-2212, 2002.

[7] Sveinsson, J., R., Benediktson, J., A.: Combined *Wavelet and Curvelet Denoising of SAR Images Using TV Segmentation.* Proceedings of IEEE IGARSS'07, pp. 503-506, 2007.

[8] Denis, L., Tupin, F., Darbon, J., Sigelle, M.: *SAR Image Regularization with Fast Approximate Discrete Minimization*. IEEE T Image Process, vol. 18, no.7, pp. 1588-1600, 2009.

[9] Yu, Y., Acton, S., T.: *Speckle Reducing Anisotropic Diffusion*. IEEE T Image Process, vol. 11, no. 11, pp. 1260-1270, 2002.

[10] Perona, P. and Malik, J.: *Scale space and edge detection using anisotropic diffusion*. IEEE T. PAMI., vol.12, pp. 629–639, 1990.

[11] Krissian, K., Westin, C.F., Kikinis, R., Vosburgh, K.: *Oriented Speckle Reducing Anisotropic Diffusion*. IEEE T Image Process, vol. 16, no. 5, pp. 1412-1424, 2007.

[12] Pollak, I., Willsky, A.,S., Krim, H.: *Image Segmentation and Edge Enhancement with Stabilized Inverse Diffusion Equations*. IEEE T. Image Process, vol.9, no.2, pp.256-266, 2000.

[13] Çetin, M., Karl, W., C.: *Feature Enhanced Synthetic Aperture Radar Image Formation Based on Nonquadratic Regularization*. IEEE T Image Proccess, vol. 10, no. 4, pp. 623-631, 2001.

[14] Tupin, F., Maitre, H., Mangin, J. F., Nicholas, J. M., Pechersky, E.*: Detection of Linear Deatures SAR Images: Application to Road Network Extraction*. IEEE T Gz Remote, vol. 36, no. 2, 1998.